BNL 745 (T-270)

325
7-18-63

# BROOKHAVEN LECTURE SERIES

# *Fundamental Studies of Radiation Damage in Graphite*

**Donald G. Schweitzer**

MASTE

Number 16

April 17, 1962

BROOKHAVEN NATIONAL LABORATORY

Associated Universities, Inc.
under contract with the
United States Atomic Energy Commission

# FOREWORD

The Brookhaven Lectures, held by and for the Brookhaven staff, are meant to provide an intellectual meeting ground for all scientists of the Laboratory. In this role they serve a double purpose: they are to acquaint the listeners with new developments and ideas not only in their own field, but also in other important fields of science, and to give them a heightened awareness of the aims and potentialities of Brookhaven National Laboratory.

Before describing some recent research or the novel design and possible uses of a machine or apparatus, the lecturers attempt to familiarize the audience with the background of the topic to be treated and to define unfamiliar terms as far as possible.

Of course we are fully conscious of the numerous hurdles and pitfalls which necessarily beset such a venture. In particular, the difference in outlook and method between physical and biological sciences presents formidable difficulties. However, if we wish to be aware of progress in other fields of science, we have to consider each obstacle as a challenge which can be met.

The lectures are found to yield some incidental rewards which heighten their spell: In order to organize his talk the lecturer has to look at his work with a new, wider perspective, which provides a satisfying contrast to the often very specialized point of view from which he usually approaches his theoretical or experimental research. Conversely, during the discussion period after his talk, he may derive valuable stimulation from searching questions or technical advice received from listeners with different scientific backgrounds. The audience, on the other hand, has an opportunity to see a colleague who may have long been a friend or acquaintance in a new and interesting light.

The lectures are being organized by a committee which consists of representatives of all departments of the Laboratory. A list of the lectures that have been given and of those which are now scheduled appears on the back of this report.

Gertrude Scharff-Goldhaber

**The drawing on the cover is taken from a 5th Century B.C. relief on the Acropolis in Athens, the "Dreaming Athena," by an unknown sculptor.**

# DISCLAIMER

BNL 745 (T-270)
(Radiation Effects on Materials; Reactor Technology – TID 4500, 17th Ed.)

# *Fundamental Studies of Radiation Damage in Graphite*

Donald G. Schweitzer

## BROOKHAVEN LECTURE SERIES

Number 16, April 17, 1962

PRINTED IN USA
PRICE 50 CENTS

Available from the
Office of Technical Services
Department of Commerce
Washington 25, D C

November 1962 1750 copies

# INTRODUCTION

It is appropriate that this lecture on radiation damage in graphite follows the lecture on water given by Dr. Allen. Both materials are considered very simple substances, but, as Dr. Allen pointed out in his lecture, water does not behave in a simple manner. After tonight's lecture I think you will see that this statement is also true for graphite. Radiation produces complex products in both these materials. It is also worth noting that water and graphite are, from a practical point of view, the two most important moderators being used in reactors throughout the world. In the United States the moderator in the commercially important reactors is water, whereas in the United Kingdom it is graphite.

The speaker for this evening is Dr. Donald G. Schweitzer. He obtained his undergraduate training at City College of New York. His graduate work was done at Syracuse University in the field of photochemistry. He joined the Metallurgy Division at Brookhaven in 1955. He has worked on the oxidation and reduction of solutes in liquid uranium-bismuth alloys, and has contributed very materially to the understanding of the films formed when steels are contacted with liquid uranium-bismuth alloys containing inhibitors. He has also made a very extensive survey of the solubilities of fission products in uranium-bismuth.

About 2½ years ago he became interested in graphite. He has already done a very important piece of work on oxidation and heat transfer in graphite channels. The lecture he will give tonight is based on his more recent studies on radiation effects on this material.

Those of us who work with Dr. Schweitzer know that he attacks a problem with vigor, enthusiasm, and imagination. He has demonstrated the ability not only to select the important experiments but also to execute them neatly. I will close this introduction by repeating something he reminded me of recently. When he first joined the group 7 years ago, I suggested a number of problems to him, and among all of them the one he said he did not want to work on was graphite. However, I think you will agree after tonight's talk that it is fortunate that he changed his mind, and that his work on graphite radiation effects has resulted in a better understanding of the effects occurring in this complex and important material.

David H. Gurinsky

# Fundamental Studies of Radiation Damage in Graphite

## CARBON AND GRAPHITE

Carbon, of all the chemical elements, is unequalled in its versatility in uses and its uniqueness in properties. The element occurs in allotropic states categorized as graphites, amorphous carbons, and diamonds, each of which includes several structural modifications. Natural graphites and diamonds can be characterized by well-defined structures, whereas amorphous carbons and synthetic graphites have neither well-defined structures nor well-defined definitions.

A schematic drawing of the diamond structure is shown in Figure 1. Diamond is a tetrahedral covalent macromolecule in which each carbon is bonded to four other carbons. Such crystals have the properties of hardness and high melting point.

The most common form of the crystalline structure of graphite is hexagonal (Figure 2). The structure of graphite is unique in that the distance between carbon atoms perpendicular to the hexagonal planes is much greater than the carbon to carbon distance within the planes. The perpendicular distance is measured by the x-ray parameter called the *C*-axis. The forces between carbon atoms in different planes arise from relatively weak Van der Waals interactions, whereas the carbon atoms in the planes are held together by strong covalent bonds. The large difference in distance between *C* and the *a* directions (Figure 2) and the variation in forces associated with the directions are responsible for the anisotropic properties of graphite, and for one of the reasons why "lead" pencils write. The multifarious properties of the different forms of carbon arise from combinations of the crystalline forms of diamond and graphite. Carbon in the form of natural graphite is one of the softest of the solid elements and in the form of diamond is the hardest. Amorphous carbon is among the best thermal insulators whereas the thermal conductivity of graphite rivals that of the best metals. Diamond is an electrical insulator and graphite is an excellent electrical conductor. Diamonds and baked carbons are abrasives while natural graphite has no substitute as a high temperature lubricant. The thermal coefficient of expansion of natural graphite is as large as that of any element in the periodic table with the exception of the alkali metals but the thermal coefficient of expansion of synthetic graphite is just about as small as that of any element. The anomalous properties of carbon are not restricted to those pertinent to the physical sciences but also appear in the fields of economics and the social sciences. As coal or coke, carbon costs about one cent per pound. Diamond, on the other hand, is somewhat more expensive, the cost going as high as a million dollars per pound. Smog and disagreeable odors in industrial areas are often attributed to gases adsorbed on soots and carbons produced by combustion of fuels. Opposing this is the use of active carbon as the most successful means of removing disagreeable odors and tastes from freshly distilled whiskies and public water supplies.

Because of the enormous and often bewildering role that carbon plays in almost every major field of science, it is not surprising that the literature is often controversial and confusing. The talk this evening will include some of our contributions to this confusion and will deal with recent studies made at Brookhaven relating to radiation damage in graphite.

## GRAPHITE AS A REACTOR MATERIAL

Some 20 years ago, when nuclear science was in its infancy, E.P. Wigner predicted that energetic neutrons resulting from the fission process would be able to displace atoms from their lattice positions in solids. A few years later Seitz and coworkers calculated the extent of such displacements and confirmed Wigner's predictions that heavy bombardment should produce important changes in properties of irradiated materials. The work prompted immediate experimental and theoretical studies on the magnitude and nature of these changes. Of particular technological concern were radiation changes induced in the materials used in nuclear reactors. In a chain reaction of the

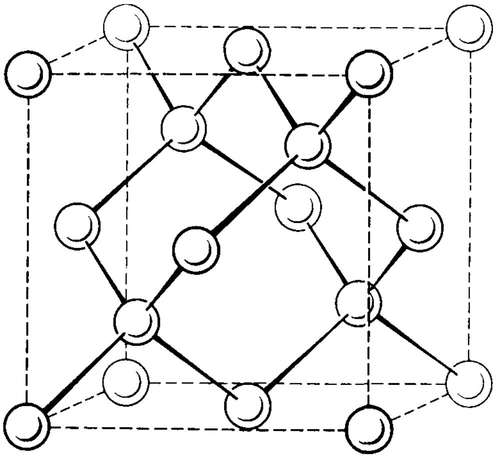

Figure 1. Crystal structure of diamond.

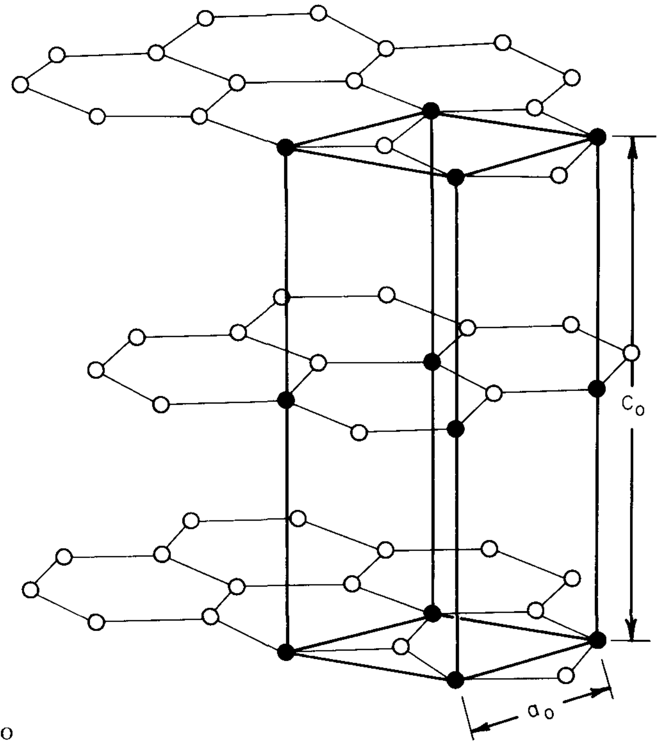

Figure 2. Crystal structure of graphite. Unit cell is accented. Normal cell dimensions: $C_0 = 6.70$ A; $a_0 = 2.46$ A.

kind used in reactors, uranium nuclei undergo fission and liberate fast neutrons. These neutrons must be slowed down by some material, called a moderator, so that they can be reabsorbed by the uranium in order to sustain the fission process. The moderator, therefore, must have the select properties of slowing down fast neutrons without absorbing too many of them. With the additional restriction that a moderator should be useful for advanced high temperature reactor concepts, graphite becomes important, since it is an excellent moderator and one of the very few structural materials that can be used at temperatures as high as 2000°C. These advantages of graphite were recognized many years ago and are responsible for the large amount of experimental work on radiation damage to this material.

A review of the literature that has accumulated during the past 20 years leaves one with the distinct impression that the studies on damage effects fall into two gross categories: one in which the experimental data seem to reflect fundamental or theoretical information on the band structure of graphite, and another composed of measurements that are complicated, are generally not reproducible, and often defy simple interpretation.

The first category seems to consist of data on electrical, magnetic, and thermal property changes, while the second includes dimensional, x-ray, and stored energy data. It is ironic that, with the possible exception of thermal conductivity, the practical problems associated with the construction and operation of reactors result from property changes included in the second category. Electrical and magnetic property changes in irradiated graphites have little effect on the engineering requirements necessary to design or operate a graphite reactor.

When irradiated at temperatures below 250° to 300°C, graphite expands. Figure 3 shows expansion vs irradiation. It can be seen that the expansion increases linearly with irradiation. Although the absolute value of the growth is small, the change is sufficient to move reactor channels out of line and thus cause trouble in loading and unloading fuel elements and experimental equipment. The change depends on the irradiation temperature, as shown in Figure 4.

Another radiation change of considerable technological importance is the development of stored energy, sometimes called Wigner's disease. Wigner predicted that neutron irradiation of graphite would increase the energy content of the lattice because of production of interstitial and vacancy defects. Wigner energy has the troublesome property of being released very rapidly at relatively low temperatures. The amount of energy (in the form of heat) released at 200°C is often great enough to increase the graphite temperature appreciably. A method of experimentally determining this release is shown in Figure 5. When unirradiated graphite

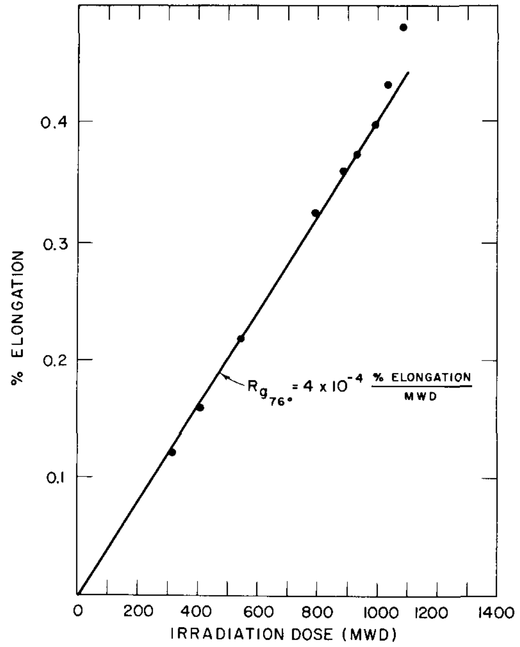

Figure 3. Rate of growth of AGOT graphite during irradiation at 76°C. (1 MWD = $7 \times 10^{16}$ nvt for neutrons with energies >0.6 Mev.)

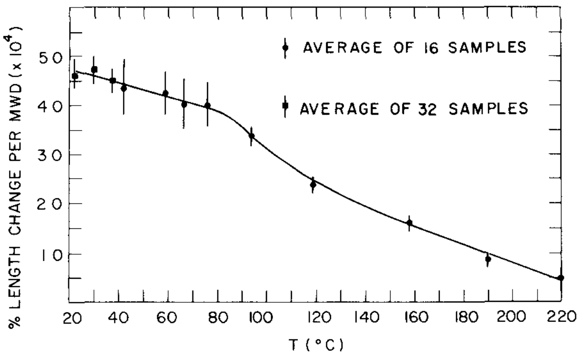

Figure 4. Rate of growth of graphite vs irradiation temperature.

is placed in a furnace held at a constant temperature (200°C in Figure 5), the graphite temperature increases with time as shown by the bottom curve. If an irradiated sample containing stored energy is similarly treated (upper curve), the temperature increases until a point is reached at which the stored energy is released. The heat resulting from the release causes the temperature of the graphite to exceed the furnace temperature until, after the completion of the release, the graphite finally cools to the temperature of the furnace.

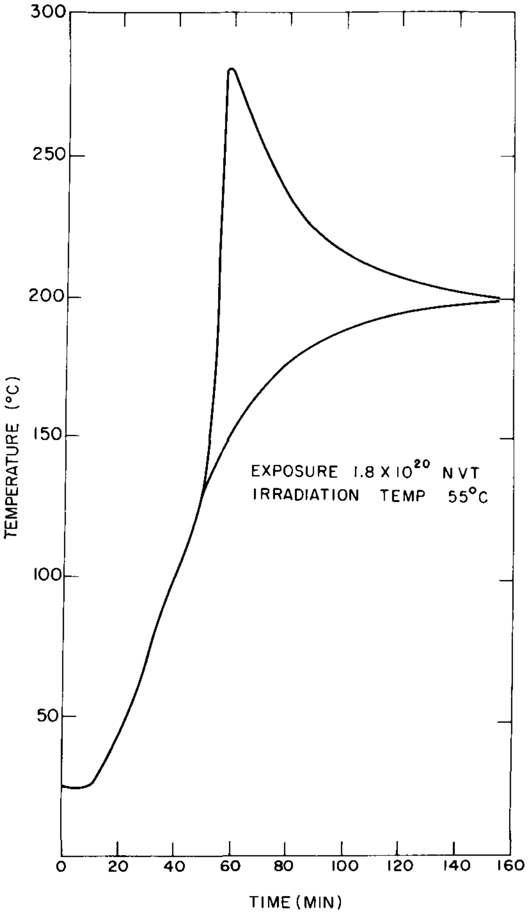

Figure 5. Low temperature energy release.

The amount of stored energy released is determined from the area between the temperature-time curves of the irradiated and unirradiated samples. Many specialists feel that this sudden release of energy could result – and, in the case of the Windscale incident, has resulted – in serious reactor accidents. Whatever the degree of danger associated with the release of stored energy, its presence is certainly undesirable.

Radiation changes such as stored energy and dimensional expansions can be removed by thermal annealing. Thermal annealing is a process in which the graphite is removed from the radiation field and heated to some temperature above the irradiation temperature, the object being to recover original properties and remove damage effects. In order to make the annealing of the graphite in the Brookhaven reactor as efficient as possible, studies were made to obtain experimental information on the nature of the reactions responsible for property changes involved in the annealing and the radiation processes. Our studies on radiation damage in graphite differ in one important respect from other studies reported. We have used the technique of frequently repeated reirradiations followed by thermal anneals, whereas almost all the data of other investigators were obtained from initial irradiations and the initial thermal anneal. The technique of measuring periodically irradiated and annealed graphite has provided information that we have used to develop a model describing the reactions occurring during the irradiation and the thermal annealing process. The model, I believe, has the advantages that it does not seem to contradict any of the established experimental observations and it can also account for many of the properties of irradiated graphite that have not been previously explained.

The remainder of this talk will deal with the novel aspects of the data and with some of the experiments from which the model was developed.

## RADIATION DAMAGE MODEL

Experimental results[1,2] indicate that the first irradiation of graphite produces only trapped single interstitials and $C_2$ molecules, in contrast to the more complicated processes usually expected. The reactions are

$$\phi + C^0 \rightarrow C_1 + \text{Vacancy}\ ; \qquad (1)$$

$$C_1 + C_1 \rightarrow C_2\ ; \qquad (2)$$

$$C_1 + \text{Trap} \rightarrow C_1T\ . \qquad (3)$$

Reaction (1) corresponds to the displacement of a lattice carbon atom to form a single interstitial ($C_1$) by collision effects of a fast (high energy) neutron ($\phi$) on the graphite lattice ($C^0$). This reaction is temperature independent. Reaction (2) represents the collision of two interstitials to form a stable $C_2$ complex. The dimensional changes (rate of growth) occurring in graphite are due to the constant (zero-order) rate of formation of $C_2$. Some of the single interstitials anneal (without causing dimensional changes) by being trapped at pores, edge atoms, etc.; reaction (3) describes this process. The rate determining step for both reaction (2) and reaction (3) is the migration of a single interstitial.

During the first thermal anneal, when the graphite temperature is raised, some of the trapped single interstitials are released and cluster randomly with the $C_2$ molecules, forming many different interstitial complexes. Property changes occurring during the first anneal are the result of reactions involving the different complexes. When the graphite is reirradiated (after 350°C thermal anneal), some of the complexes decompose and some form by reactions such as

$$C_n + C_1 \rightleftarrows C_{n+1}\ , \qquad (4)$$

$$C_{n+1} + C_1 \leftrightarrows C_{n+2}\ , \qquad (5)$$

$$C_a + C_1 \rightleftarrows C_{a+1}\ , \qquad (6)$$

where the subscripts refer to the number of carbon atoms in the complex. Since the above reactions lead to specific distributions of complexes, the subsequent thermal anneals differ from the first in that the changes are due to reactions involving different concentrations of interstitial species.[10]

Thermal annealing appears to involve the three types of reactions given by

$$C_n \rightarrow aC_2 + bC_1 \qquad (7a)$$

(where $n = 2a + b$), or possibly

$$C_n \rightarrow xC_2 + yC_1 + C_m \qquad (7b)$$

(where $n = m + 2x + y$) ;

$$C_2 + \text{Trap} \rightarrow C_2T\ , \qquad (8a)$$

$$C_1 + \text{Trap} \rightarrow C_1T\ ; \qquad (8b)$$

$$C_x + C_2 \rightarrow C_{x+2}\ , \qquad (9a)$$

$$C_x + C_1 \rightarrow C_{x+1}\ . \qquad (9b)$$

Reactions (7a) and (7b) represent the decomposition of interstitials into smaller species. The mobile species ($C_1$, $C_2$, etc.) can either anneal [reactions (8a) and (8b)] or combine with different complexes ($C_x$) to form new complexes ($C_{x+1}$, $C_{x+2}$) that are stable at the temperature of the anneal. The latter reactions are reclustering reactions which result in redistribution of damage or production of new damage.

## INITIAL IRRADIATION

The first group of experiments to be discussed were used to obtain information on reactions (1), (2), and (3) describing the first irradiation. The techniques applied to dimensional and *C*-axis expansions were used to obtain an experimental determination of the diffusion energy of a single interstitial and the absolute rate of forming displaced atoms

One of the key problems in radiation damage to graphite is the identification of annealing reactions of the single interstitial At present no experimental evidence exists that clearly indicates how or under what conditions a single interstitial is removed from an irradiated graphite lattice We have approached the problem by means of the following argument

When neutrons of high energy collide with lattice atoms, the rate of displacement of the atoms is dependent on flux intensity but should not be dependent on sample temperature because of the high energies involved A displaced atom (interstitial) of high energy will undergo many collisions rapidly, until its energy is reduced to values corresponding to the lattice temperature During this process some interstitials will remain in stable configurations and some will anneal out immediately The interstitials that do not anneal cause an increase in the dimensions of the sample A good deal of evidence[3 4] indicates that the dimensional increases are directly proportional to the concentration of these interstitials Thus, the difference between the absolute rate of formation of displaced atoms and the rate of dimensional change at any temperature is a measure of the rate of annealing of interstitials at that temperature The rate of annealing at temperature $T$, or $R_{a(T)}$, is then given by

$$R_{a(T)} = \bar{K} - R_{g(T)} \qquad (10)$$

where $\bar{K}$ can be considered as the maximum or absolute rate of growth for the particular type of graphite (It should be noted that $\bar{K}$ is expressed in the same units as $R_g$, i e , change per MWD, and is therefore normalized for flux intensity )

In order to obtain the activation energy for the annealing process, a value of $\bar{K}$ must be selected to give a straight line on an Arrhenius plot (This treatment assumes the rate of annealing to be an exponential function of temperature ) No straight line is obtained until the value selected for $\bar{K}$ exceeds 2 2 times the growth rate at 30°C For increasing values of $\bar{K}$ above 2 2 $R_{g(30\ C)}$, a series of straight lines are obtained with activation energies that decrease as $\bar{K}$ is increased A reasonably precise value of $\bar{K}$ can be selected if the data are required to account for the rate of growth over a large irradiation temperature interval Keating's[7] work shows that the growth rate at room temperature is ½ the growth rate at 77°K to obtain a single activation energy for irradiations from 77°K to 490°K, the value of $\bar{K}$ is found to be 2 5 times the rate of growth at 30°C The corresponding activation energy is then 0 034 ev The rate of annealing at some temperature $T$ can now be given as

$$R_{a(T)} = 2\ 5 R_{g(30\ )} - R_{g(T)} \qquad (11)$$

where $R_g$ is in percent expansion per MWD

An Arrhenius plot of $R_a$ vs $1/T$ for $\bar{K} = 2\ 5\ R_{g(30^\circ)}$ is shown in Figure 6 along with a similar plot obtained from Hanford data [8 9] (In Figures 6 and 7 the ordinate functions have been multiplied by 2

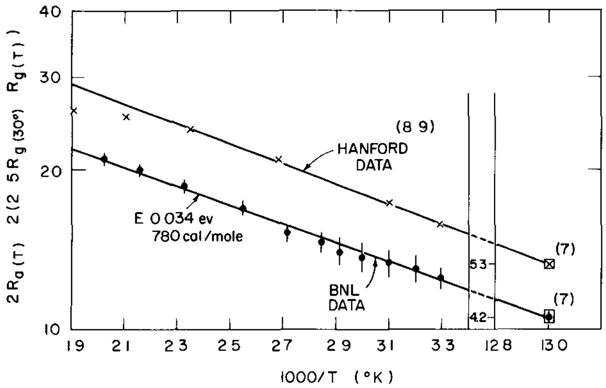

Figure 6 Rate of annealing of single interstitials vs temperature

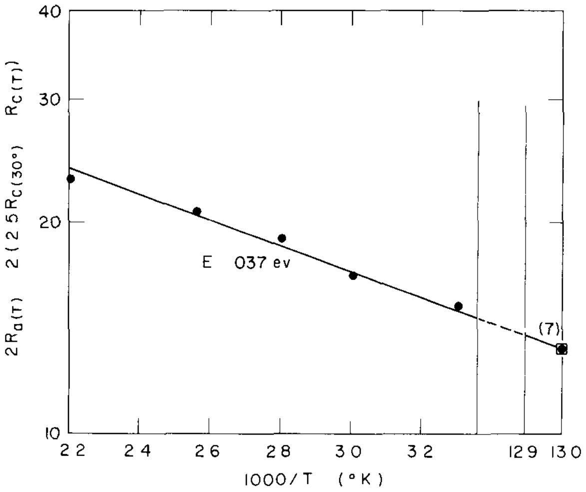

Figure 7 Rate of annealing of single interstitials from C-axis expansions

so that the data could be plotted on 1-cycle semilog paper.) Although the rate of growth of the Hanford graphite is different from that of Brookhaven graphite, the curves are in good agreement, in both cases indicating that the maximum rate of growth for a graphite is about 2.5 times its rate of growth at 30°C.

The same activation energy and absolute rate of formation of displaced atoms obtained from the temperature dependence of the growth rates can also be obtained from the temperature dependence of the rate of *C*-axis expansion. Earlier work done at Brookhaven indicated that the *C*-axis expansion was linear with irradiation to at least 500 MWD. We have found, in agreement with this work, that although the rate of *C*-axis expansion is about 10 times the rate of dimensional expansion, the temperature dependences of both properties are the same. Figure 7 shows the rate-of-annealing function ($\bar{K}-R_{C\ \mathrm{axis}(T)}$) vs the reciprocal of the irradiation temperature. The function was calculated in the same way as Equation (11). The rate of *C*-axis expansion at 77°K is twice the rate of expansion at room temperature.[7] The absolute rate of *C*-axis expansion ($\bar{K}$) necessary to obtain the linear Arrhenius plot is again shown to be 2.5 times the rate at 30°C. The activation energy obtained from the *C*-axis data (0.037 ev) is in excellent agreement with the activation energy (0.034 ev) obtained from the dimensional expansion data.

Dienes[5] has shown that the rate of production of displaced atoms at 30°C is about $2\times10^{-3}$%/MWD. The absolute rate ($\bar{K}$) is then equal to $5\times10^{-3}$% displaced atoms per MWD.

## RADIATION GROWTH MECHANISM

The radiation growth mechanism which yields kinetic equations in agreement with the experimental Equation (10) is that given by Equations (1) to (3):

$$\phi+\mathrm{C}^{\circ}\xrightarrow{\bar{K}}\mathrm{C}_1+\text{Vacancy}\ ; \qquad (1)$$

$$\mathrm{C}_1+\mathrm{C}_1\xrightarrow{k_2}\mathrm{C}_2\ ; \qquad (2)$$

$$\mathrm{C}_1+\text{Trap}\xrightarrow{k_3}\mathrm{C}_1\mathrm{T}\,. \qquad (3)$$

Reaction (1) represents the temperature independent absolute rate of formation of displaced atoms (single interstitials). The rate of growth ($R_g$) is due to the formation of $\mathrm{C}_2$, or

$$R_g=d\mathrm{C}_2/dt\,. \qquad (12)$$

The rate of annealing of single interstitials during the irradiation is given by reaction (3), where T represents various types of trapping sites with no energy barriers. The concentrations of these traps are assumed to be fixed. The activation energy for reactions (2) and (3) is therefore the migration energy of the single interstitial.

At steady state the single interstitial concentration does not change and

$$d\mathrm{C}_1/dt=\bar{K}-k_2\mathrm{C}_1{}^2-k_3\mathrm{C}_1=0\,. \qquad (13)$$

The rate of growth ($R_g$) is then

$$d\mathrm{C}_2/dt=k_2\mathrm{C}_1{}^2\,. \qquad (14)$$

Solving for $\mathrm{C}_1$ and substituting in Equation (14) gives

$$d\mathrm{C}_2/dt=(1/4k_2)[2k_3{}^2+4k_2\bar{K}-2k_3(k_3{}^2+4k_2\bar{K})^{1/2}]. \qquad (15)$$

It can be shown that $4k_2\bar{K}>k_3{}^2$ over 80% of the total annealing range (irradiation temperatures from 77° to about 420°K) and the ratio $4k_2\bar{K}/k_3{}^2$ is independent of the steady state concentration ($\mathrm{C}_1$). For example, for $\bar{K}=5\times10^{-3}$% displaced atoms/MWD and $R_g=3\times10^{-3}$% displaced atoms/MWD,

$$d\mathrm{C}_2/dt=3\times10^{-3}\%=k_2\mathrm{C}_1{}^2\,. \qquad (16)$$

If $\mathrm{C}_1=10^{-5}$%, then $k_2=3\times10^7$.

Substituting for the above values in Equation (13) gives

$$k_3\mathrm{C}_1=2\times10^{-3}\%\,, \quad \text{or} \quad k_3=2\times10^2\,. \qquad (17)$$

The ratio

$$4k_2\bar{K}/k_3{}^2=4\times3\times10^7\times5\times10^{-3}/(2\times10^2)^2=15.$$

Similarly, if $\mathrm{C}_1=10^{-8}$%, then

$$k_2=3\times10^{13}, \quad k_3=2\times10^5$$

and

$$4k_2\bar{K}/k_3{}^2=4\times3\times10^{13}\times5\times10^{-3}/(2\times10^5)^2=15\,.$$

Neglecting the second-order $k_3$ terms, Equation (15) reduces to

$$d\mathrm{C}_2/dt=(1/4k_2)[4k_2\bar{K}-2k_3(4k_2\bar{K})^{1/2}] \qquad (18)$$

or

$$d\mathrm{C}_2/dt=\bar{K}-(\bar{K}/k_2)^{1/2}k_3\,. \qquad (19)$$

With the rate constants expressed as exponentials,

$$k_2=k_0e^{\ E/RT}\ , \qquad (20)$$

$$k_3=k_0'e^{-E/RT} \qquad (21)$$

(where $E$ is the migration energy of the single interstitial).

The temperature dependence of the rate of growth obtained by substitution of Equations (20) and (21) into Equation (19) gives

$$dC_2/dt=\bar{K}-(\bar{K}/k_0)^{1/2}k_0'e^{(\ E+F/2)/RT} \qquad (22)$$

or

$$R_g=\bar{K}-k_4e^{(\ E/2)/RT}\ . \qquad (23)$$

From Equation (10) the rate of annealing ($R_a$) is therefore

$$R_a=k_4e^{(\ E/2)/RT}=\bar{K}-R_g \qquad (24)$$

where (from Figure 6) $E/2=0.034$ ev and $E=0.068$ ev.

In the above model, the formation of $C_2$ is necessary to fit the derived kinetic equations with the experimental results. Similar mechanisms in which the dimensional changes are assumed to be due to a particular type of trapped single interstitial do not yield a temperature dependence for the rate of growth.

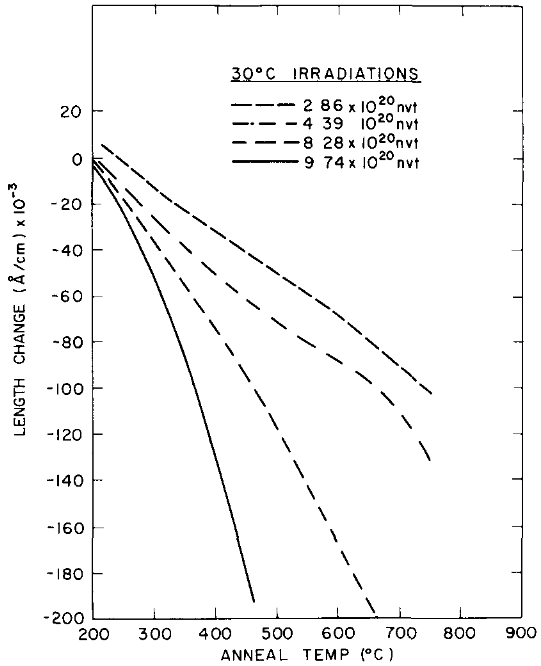

Figure 8 Dimensional changes after the first thermal anneal

If the mechanism is

$$\phi+C^{\circ}\xrightarrow{\bar{K}}C_1+\text{Vacancy}\ , \qquad (25)$$

$$C_1\xrightarrow{k_2}C_1{}^*\quad\text{(dimensional increase)}\ ; \qquad (26)$$

$$C_1+T\xrightarrow{k_3}C_1T\quad\text{(no dimensional changes)}; \qquad (27)$$

then the steady state equation is first-order with $C_1$, or

$$dC_1/dt=\bar{K}-k_2C_1-k_3C_1=\bar{K}-k_1C_1\ . \qquad (28)$$

The rate of growth is therefore

$$dC_1{}^*/dt=k_2C_1\ . \qquad (29)$$

$C_1$ will build up exponentially to the steady state concentration $\bar{K}/(k_2+k_3)$, and Equation (29) becomes

$$dC_1{}^*/dt=\bar{K}k_2/(k_2+k_3)\ . \qquad (30)$$

Since reactions (26) and (27) should have the same activation energy, the rate of growth will have no temperature dependence and is given by

$$dC_1{}^*/dt=\bar{K}\,k_0e^{\ E/RT}/(k_0+k_0')e^{\ E/RT}=\bar{K}k_0/(k_0+k_0')\ . \qquad (31)$$

Mechanisms involving the formation of a complex $C_n$ (where $n>2$) result in higher-order differential equations. Steady state assumptions cannot be justified if additional reactions such as

$$C_2+C_1\rightarrow C_3 \qquad (32)$$

are used. The resulting differential equations cannot be solved in closed form and do not appear to reduce to equations similar to Equation (23).

## REIRRADIATION REACTIONS

The next group of experiments to be described were used to obtain information that indicates that equilibrium reactions between interstitials occur during reirradiations.

Typical data from the first thermal annealing of neutron irradiated graphites show that the greater the irradiation dose, the greater is the recovery obtained at a given temperature. Dimensional changes occurring during the anneal result from continuous recovery associated with continuous increase in temperature. An example of these effects is shown in Figure 8. The total concentration of interstitial complexes and, very likely, the concentration of any particular species formed by a clustering reaction during an anneal should depend on the concentration of trapped single interstitials and $C_2$ molecules present in the graphite. The concentration of these will, in turn, depend on the initial irradiation dose, so that increasing recoveries are to be expected with increasing irradiations. The monotonic nature of the annealing implies that a variety of interstitials are formed that anneal at different temperatures.

When graphites containing complexes that anneal over a temperature continuum are reirradiated and annealed again, the monotonic nature of the annealing is removed and the discrete annealing shown in Figure 9 is observed. Annealing curves of periodically irradiated graphites show temperature regions in which almost no dimensional recovery is observed, suggesting that the concentrations of the complexes that anneal in these regions in continuously irradiated graphites are markedly reduced in the periodically irradiated material. The data given in Figure 9 show that after a 350°C anneal only one complex that anneals below 350°C is formed when the reirradiation is 15 MWD or less. Increasing the reirradiation produces at least two more complexes that anneal below 350°C (Figure 10). In none of the samples studied has recovery been observed at 250°C without corresponding recovery at 110°C. The observation implies that the complex that anneals at 250°C may be formed from the complex that anneals at 110°C.

Radiation removal of complexes that anneal between 110°C and 250°C and between 250°C and 300°C may result from decomposition due to direct collisions of fast neutrons and the missing complexes by reactions such as

$$C_n+\phi\rightarrow nC_1 \tag{33}$$

or

$$C_n+\phi\rightarrow C_a+C_b+C_c+C_1 \tag{34}$$

where $a+b+c+1=n$, followed by

$$C_1+\text{Trap}\rightarrow C_1T\,. \qquad (35)^1$$

Decomposition may also occur in the absence of direct collision from thermal effects of energetic neutrons by reactions such as

$$C_n \xrightarrow{\phi} C_{n-1}+C_1 \tag{36}$$

followed by reaction (35).

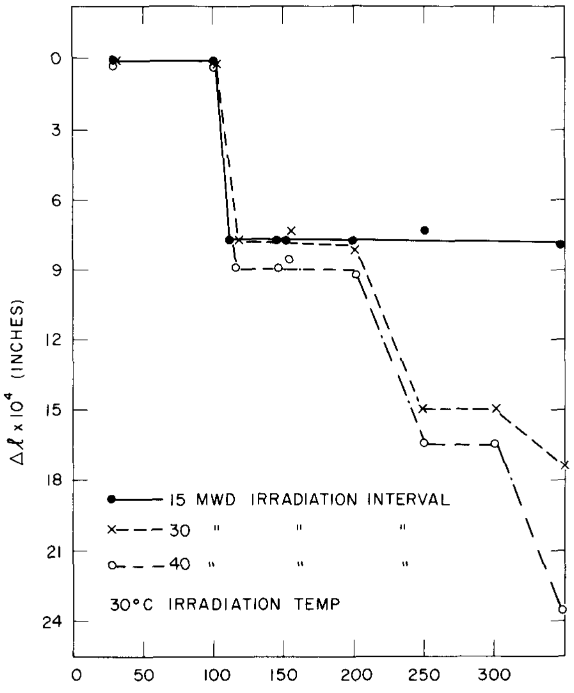

Figure 9. Dimensional recoveries (contractions) for periodically irradiated graphite.

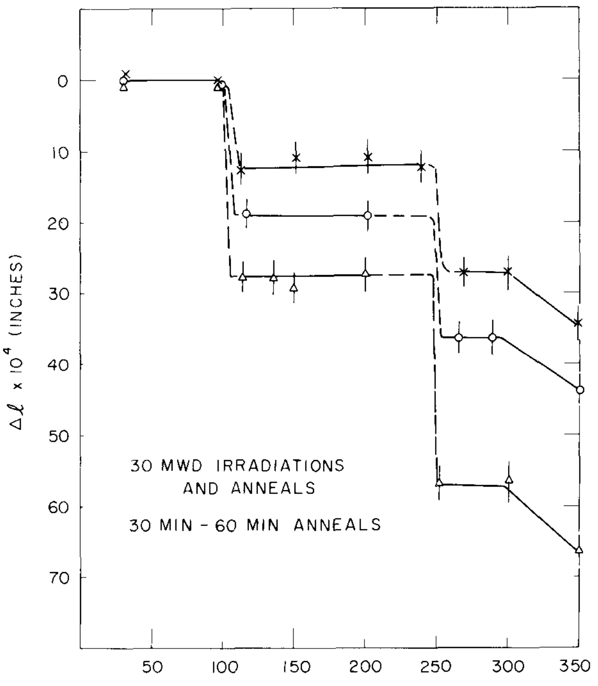

Figure 10. Dimensional recoveries (contractions) for periodically irradiated graphite.

In graphites containing about 1% interstitials, the probability of direct collision is small, so that most of the radiation decomposition may be expected from thermal spike effects. Because of the high local temperatures in the thermal spike regions, all complexes should be subject to such decomposition reactions. However, some of the interstitial complexes may act as trapping sites for the single interstitials produced by the primary irradiation process, leading to competing formation reactions such as

$$\phi + C^0 \rightarrow C_1 + \text{Vacancy}\,, \qquad (37)$$

$$C_{n-1} + C_1 \rightarrow C_n\,. \qquad (38)$$

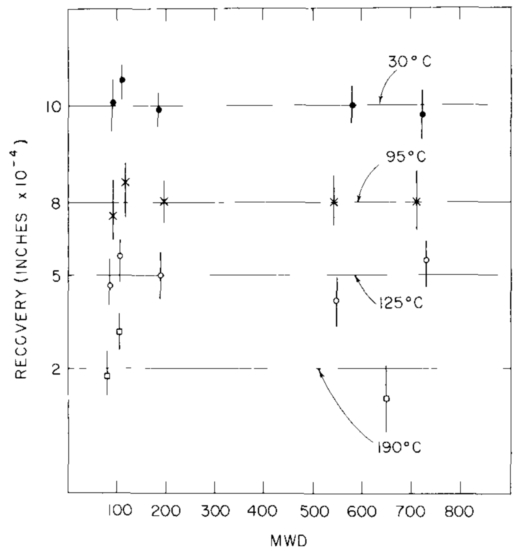

Figure 11. Absolute recovery values (for 4-in. samples) vs irradiation interval at various irradiation temperatures.

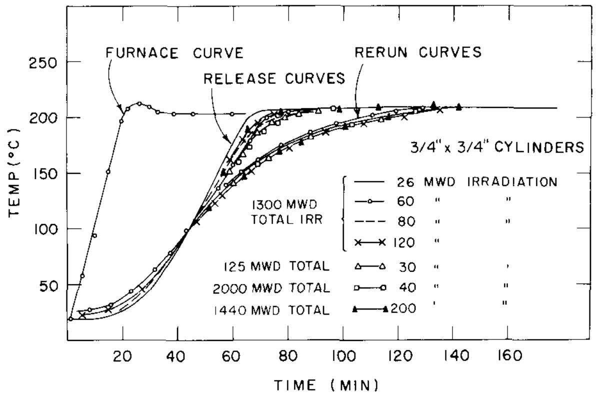

Figure 12. Stored energy released at 200°C.

Similarly, if $C_n$ as well as $C_{n-1}$ is a trapping site, consecutive formation reactions such as

$$C_{n-1} \xrightarrow{C_1} C_n \xrightarrow{C_1} C_{n+1} \rightarrow \text{etc}\,. \qquad (39)$$

may occur competing with the radiation decomposition reactions. The net effect of the reirradiation reactions should be the eventual reduction in concentration of those interstitials that have small binding energies. The formation reaction, (38), and the decomposition reactions, (36), for complex $C_n$ will depend on the concentrations of $C_{n-1}$, $C_n$, and $C_{n+1}$. After some time, when the rate of formation of $C_n$ equals its rate of removal, $C_n$ will be in a steady state given by

$$\ldots \underset{\phi}{\overset{C_1}{\rightleftarrows}} C_{n-1} \underset{\phi}{\overset{C_1}{\rightleftarrows}} C_n \underset{\phi}{\overset{C_1}{\rightleftarrows}} C_{n+1} \underset{\phi}{\overset{C_1}{\rightleftarrows}} \ldots\,. \qquad (40)$$

In contrast to the effects observed in continuously irradiated graphites, reaction (40) requires that the concentration of a particular species in periodically irradiated graphites should no longer increase with irradiation interval beyond the period necessary to reach steady state.

Measurement of dimensional changes resulting from the annealing of different complexes is one of the techniques that can be used to demonstrate the above steady state concentrations. In Figure 11 it can be seen that all the complexes that anneal below 350° reach steady state conditions beyond 60 MWD of irradiation and thereafter do not change as they do in continuously irradiated samples.

The release of stored energy accompanying dimensional and *C*-axis changes is another property that demonstrates steady state interstitial concentrations. Again in marked contrast to the effects observed in continuously irradiated graphites, the steady state reactions result in stored energy releases that do not increase with irradiation beyond the steady state value. The steady state value of the 200°C stored energy release is shown in Figure 12. It is immediately obvious that in periodically irradiated graphites the 200°C stored energy no longer increases with irradiation as it does in continuously irradiated graphites. Both the initial release temperature and the reirradiation necessary to reach steady state are in excellent agreement with the dimensional studies for the complex that anneals at 110°C.

In addition to consecutive reactions such as those represented by reaction (40), steady state might result from isolated reactions such as

$$C_a \xrightleftharpoons[\phi]{C_1} C_{a+1} \,, \tag{41}$$

$$C_b \xrightleftharpoons[\phi]{C_1} C_{b+1} \,. \tag{42}$$

Reactions (41) and (42) will occur if complexes $C_{a-1}$, $C_{b-1}$, $C_{a+2}$, and $C_{b+2}$ are unstable and if $C_a$ and $C_b$ are initially formed during an anneal.

If complexes which are chain initiating species (i.e., $C_a$, $C_b$) are removed by a thermal anneal, the initial effects expected during the reirradiations should be the decomposition of the larger species in order to re-establish steady state. The decomposition reactions result in radiation contraction effects that are not observed in continuously irradiated graphites. These contraction effects are shown in Figure 13 for graphites irradiated regularly at 30° to 80°C and then reirradiated (after a 350°C anneal) at 30° to 50°C for the small intervals shown.

If the majority of interstitials are involved in isolated reactions such as those given by reactions (41) or (42), removal of a limited number of species (i.e., $C_a$, $C_b$) by a 350°C anneal might at first lead to a reduction in dimensions due to decomposition of $C_{a+1}$ and $C_{b+1}$. However after all of $C_{a+1}$ and $C_{b+1}$ are removed, further irradiation should lead to dimensional expansion through formation of $C_2$ by the primary process or by complex formation at the ends of chains such as given by reaction (40). Experimentally, it is found that graphites reirradiated less than 80 MWD show continuous reduction in dimensions when the sample is annealed at 350°C after each irradiation. Figure 14 shows typical data of the dimensional changes resulting from 350°C anneals for different irradiations. The linear portion of the curve from 0 to about 1000 MWD shows the expansion before the first anneal. The middle portion of the curve shows the changes after 350°C anneals when the annealing frequency was the same as that used to anneal the Brookhaven reactor. It can be seen that the dimensions of the sample are reduced continuously when the annealing follows short reirradiations. The almost constant value of the reduction in dimensions obtained after each irradiation and annealing cycle suggests that the contraction is not due to decomposition reactions such as reactions (33) or (34). Reaction (33) should be dependent on the residual interstitial concentration and would lead to dimensional contractions showing a dependence on the residual dimensional damage. Similar arguments hold for reaction (34).

The evidence from which the irradiation reactions have been set up implies that only single interstitials are mobile at the temperatures investigated. The principal mode of formation of one complex from another is therefore assumed to result from collision reactions between immobile clusters and mobile single interstitials and not from consecutive reactions such as

$$C_n \xrightleftharpoons[\phi]{C_2} C_{n+2} \xrightleftharpoons[\phi]{C_2} C_{n+4} \tag{43}$$

or isolated reactions such as

$$C_a \xrightleftharpoons[\phi]{C_2} C_{a+2} \,. \tag{44}$$

On the other hand, decomposition resulting from neutron bombardment should occur through many

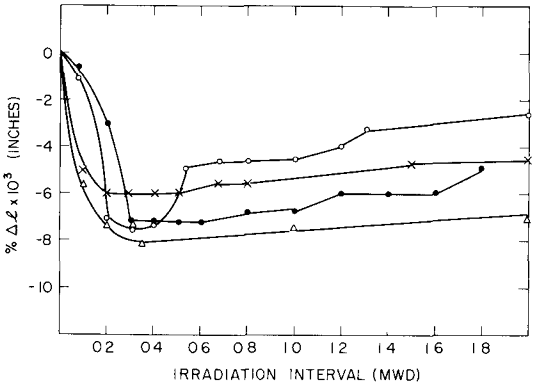

Figure 13. 30°C irradiation contraction (after a 350°C anneal).

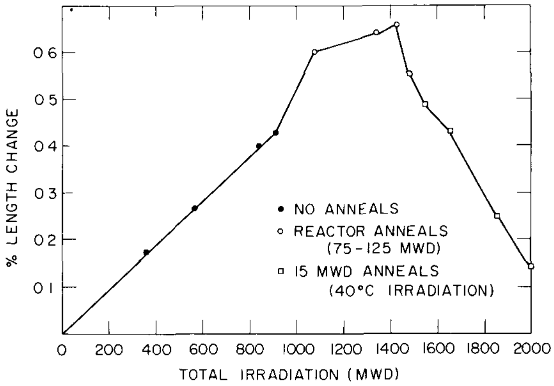

Figure 14. Dimensional changes vs annealing procedures at 350°C.

different processes such as reactions (33), (34), and (36). Although reactions (33) and (34) may occur during the first reirradiations, the evidence indicating steady state reactions and the almost constant recoveries obtained in a given sample for very large differences in total interstitial concentration (Figure 14) indicate that reactions (33) and (34) become unimportant relative to reactions such as (40).

Experimentally, the concentration of the complex that anneals at 110°C is found to remain almost constant independent of large changes in the total interstitial concentration and the complex that anneals at 250°C appears to form from the 110°C complex. If these complexes are produced from formation reactions,

$$C_x \xrightarrow{C_1} C_{110^\circ} \xrightarrow{C_1} C_{250^\circ}, \tag{45}$$

then removal of $C_{110^\circ}$ and $C_{250^\circ}$ by a thermal anneal should not result in total contraction of the sample as shown in Figure 14. If it is assumed that the only radiation reaction is (45), then the anneal would result in removing 100% of all the growth. Additional formation reactions would lead to expansion of the graphite when the other products do not anneal below 350°C. However, if the complex that anneals at 110°C is a species at the low end of a chain, the contraction shown in Figure 14 implies that the rate of decomposition of the species producing 110° complex through a chain,

$$C_{x+1} \underset{C_1}{\overset{\phi}{\rightleftarrows}} C_x \underset{C_1}{\overset{\phi}{\rightleftarrows}} C_{x-1} \underset{C_1}{\overset{\phi}{\rightleftarrows}} C_{110^\circ} \underset{C_1}{\overset{\phi}{\rightleftarrows}} C_{250^\circ}, \tag{46}$$

is greater than the rate of formation of the largest species on the chain. The constant recoveries at 110°C imply that the concentration of the species decomposing to form the 110°C complex also remains constant. The effect suggests that the decomposition reactions are fast relative to the formation reactions so that the intermediate species in a chain rapidly attain equilibrium and their concentrations effectively remain constant when one end of the chain is removed. Thus the removal of the smallest species by thermal annealing indirectly removes the largest species while intermediate complexes remain in steady state concentrations.

The large amount of dimensional damage that can be removed by repeated thermal annealing of only a single complex suggests that most of the complexes are in equilibrium through a single integral chain. Kinetic calculations of such consecutive reaction systems[6] appear to support the experimental results.

## ANNEALING REACTIONS

The final group of experiments to be summarized deals with the reactions occurring during the annealing process. These experiments will be used to demonstrate the following: (1) that thermal annealing not only removes damage but redistributes and creates it, (2) that reclustering reactions can be demonstrated experimentally, (3) that the assumption that single interstitials anneal by annihilating vacancies leads to a specific type of reaction releasing stored energy, and (4) that high temperature stored energy releases are not always the result of annealing mobile vacancies.

The first effect one might expect from random reclustering reactions is removal of some of the discrete annealing properties. In addition, if the new complexes formed during thermal reclustering contribute larger property changes per carbon atom than the complexes from which they were formed, damage can be created by reclustering and reverse annealing should occur. Both these effects can be seen in Figure 15, which shows the occurrence of dimensional expansion rather than contraction. Similar reverse *C*-axis annealing is shown at a different temperature in Figure 16.

In an attempt to assign stored energy releases to one of the annealing reactions, (7), (8), or (9), stored energy distributions were determined on samples that showed reverse annealing.

Suppose that stored energy results only from the annihilation reactions (8a) and (8b) and that the traps are vacancies so that the reactions are not reversible. Reclustering then can at most reduce stored energy releases from these reactions to zero but could not produce reverse stored energy annealing. Reverse stored energy annealing is, however, observed experimentally, as shown in Figures 17 and 18. If stored energy releases result from a single type of reaction, it is noteworthy that the above experiments require the release to be a measure of the exothermic heat of decomposition of a complex, since heat releases resulting from the formation of a new complex would show an inverse relationship between dimensional and stored energy annealing. Thus the assumption that the

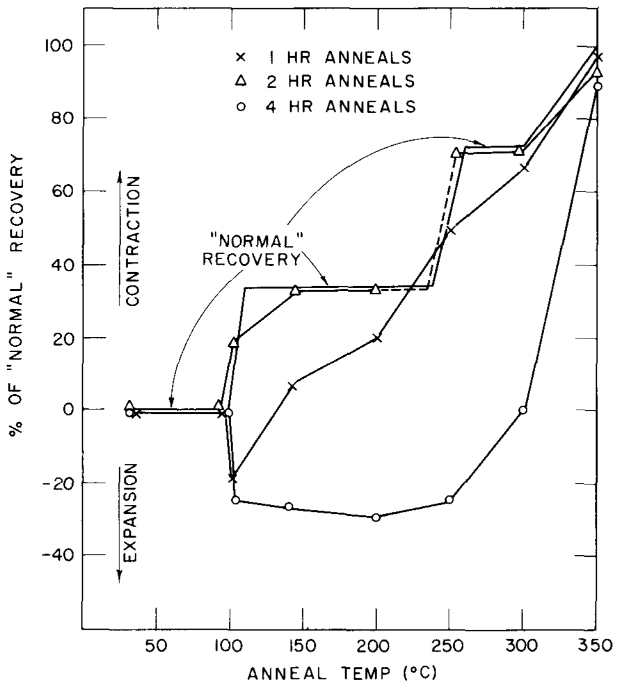

Figure 15. Reverse dimensional annealing

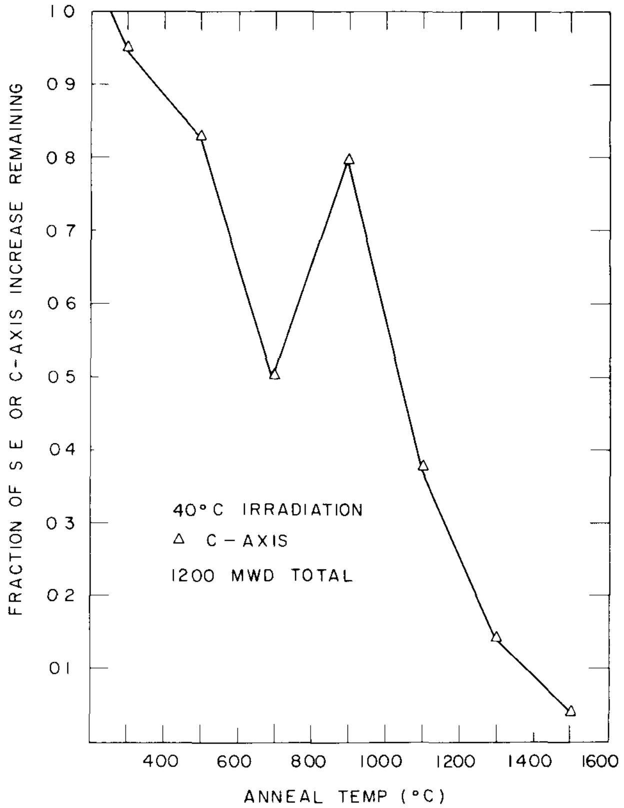

Figure 16. Reverse *C*-axis annealing.

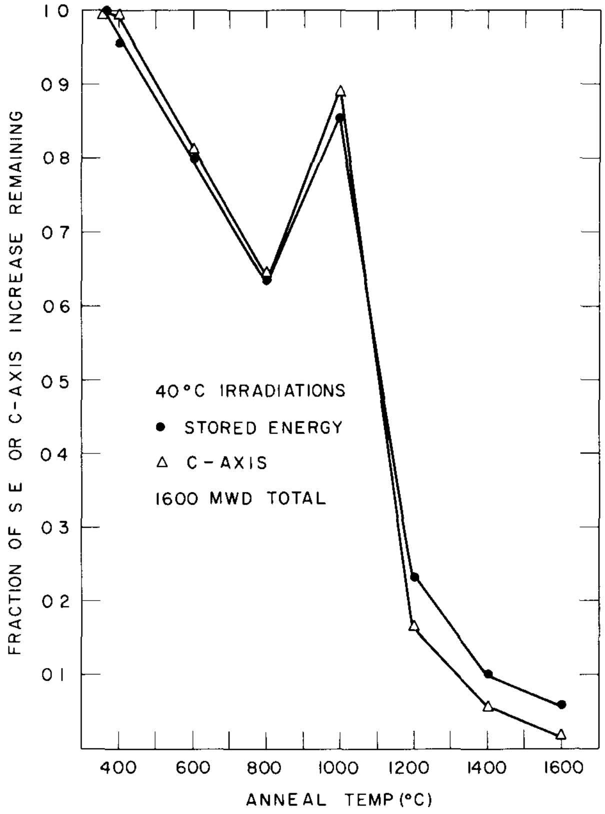

Figure 17. Reverse stored energy and *C*-axis annealing.

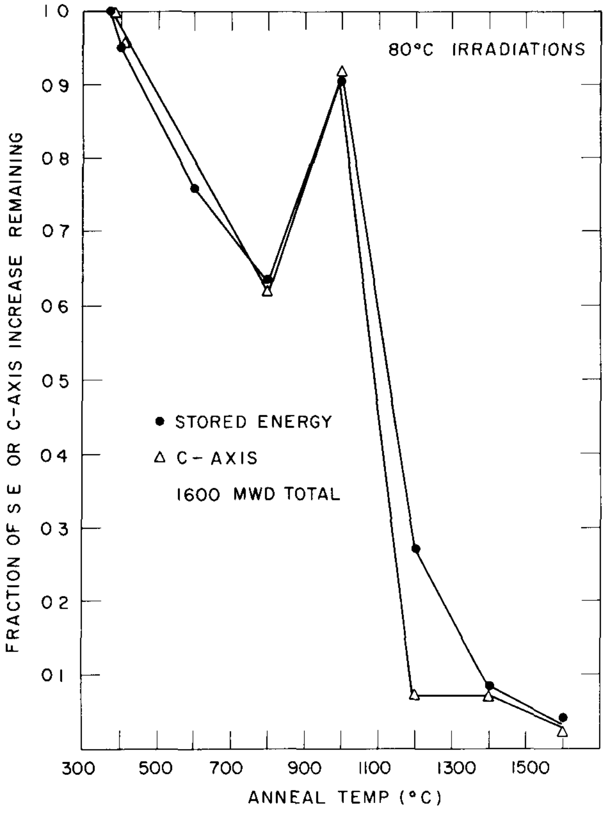

Figure 18. Reverse stored energy and *C*-axis annealing.

annihilation reactions (8a) and (8b) are so stable that they cannot be reversed leads to the apparent contradiction that little or none of the stored energy results from this reaction. In addition, the assumption requires that the new complexes formed when reverse stored energy annealing occurs are metastable, since they absorb energy from the furnace at a low temperature and release it at a higher temperature.

An alternative explanation of stored energy releases can be postulated if it is assumed that the trapped single interstitials do not recombine with vacancies and that reactions (8a) and (8b) can be reversed by raising the temperature. Under these conditions annealing reactions (with $E$=energy in the form of heat) can be described by

$$E_1+C_1T_1\rightarrow C_1 \quad \text{(mobile)}\,, \tag{47}$$

$$C_1+T_2\rightarrow C_1T_2+E_2\,, \tag{48}$$

$$C_1+C_n\rightarrow C_{n+1}+E_3 \quad \text{(dimensional increase)}\,, \tag{49}$$

followed by the higher temperature reactions

$$E_4+C_{n+1}\rightarrow(n+1)C_1\,, \tag{50}$$

$$(n+1)C_1+(n+1)T_3\rightarrow(n+1)C_1T_3+E_5\,. \tag{51}$$

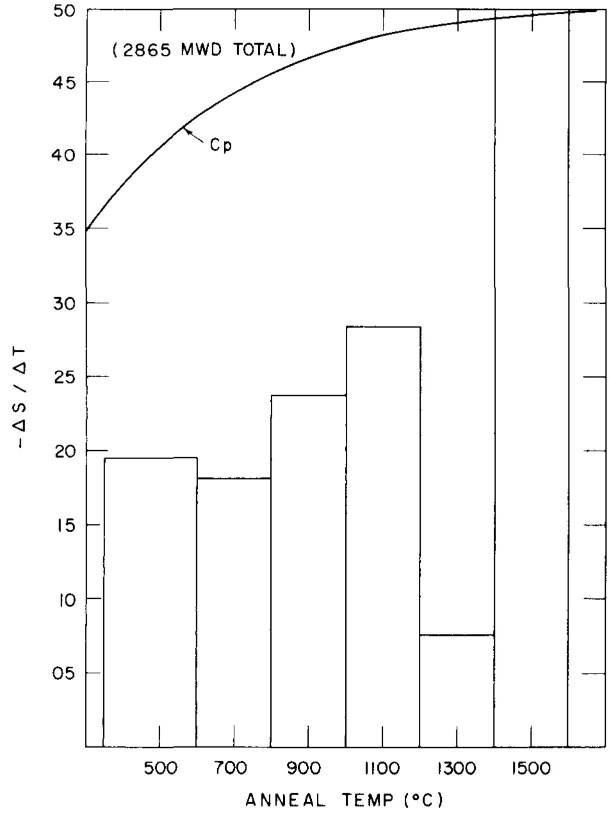

Figure 19. Stored energy distribution in BGRR graphite.

Normal annealing (contraction) accompanied by a stored energy release would involve reactions (47), (48), (50), and (51), where $E_2+E_5>E_1+E_4$ and the dimensional decrease is due to decomposition of $C_{n+1}$ followed by removal of the $C_1$ [reaction (51)]. Reverse stored energy and reverse dimensional annealing (expansion) would result from reactions (47) and (49) if $E_1>E_3$.

The latter description of annealing reactions seems the more reasonable of the two, in that the annihilation reaction and the formation of the stable larger complexes are accompanied by energy releases.

The last experiment will be interpreted as resulting from all the annealing effects just described. Reclustering effects can be demonstrated by reverse annealing experiments when the damage properties of the new complexes are greater than those of the complexes from which they are formed. In the absence of measurable reverse annealing, reclustering should nevertheless lead to redistribution of damage so that the damage spectrum in periodically irradiated graphites may be considerably different from that in continuously irradiated graphite. Figure 19 shows such effects on the stored energy distribution. The data are significant in that the total amount of stored energy making up the curve is about ½ of what it would be in a similar piece of graphite that was continuously irradiated. A very striking difference also exists in the amount of stored energy released at 1400° to 1600°C. In this graphite the high temperature stored energy content is about 10 times as much as would be present in continuously irradiated graphite. In addition to demonstrating redistribution effects, the results indicate that much of the release in this temperature region is not due to vacancy annealing. Periodically irradiated and annealed graphites should have less of a vacancy concentration than continuously irradiated graphites. In spite of this, the stored energy release at 1400° to 1600°C is about 10-fold greater, which indicates that most of the high temperature release is due to interstitial annealing and not vacancy annealing.

In conclusion, our results indicate that the irradiation reactions are simpler, the annealing reactions are more complicated, and the stored energy reactions are different from the reactions assumed by other investigators.

## REFERENCES

1 D G Schweitzer, The activation energy for annealing single interstitials in neutron irradiated graphite and the absolute rate of formation of displaced atoms, *Phys Rev* **128**, in press (October 1962)

2 D G Schweitzer, Radiation damage in graphite, I Consecutive and steady state reactions of interstitial complexes, *J Chem Phys*, in press

3 G R Hennig and J E Hove, *Proc Intern Conf on Peaceful Uses of Atomic Energy*, Vol 7, p 666 (Paper No 751), UN, New York, 1956

4 W K Woods, L P Bupp, and J F Fletcher, *ibid*, p 455 (Paper No 746)

5 G J Dienes and G H Vineyard, *Radiation Effects in Solids*, Interscience, New York, 1957

6 D G Schweitzer, Radiation damage in graphite, III Interstitial reaction kinetics comparison of theory and experiment, *J Chem Phys*, in press

7 D T Keating, *Phys Rev* **98**, 1859 (1955)

8 R E Nightingale et al , *Proc 2nd UN Intern Conf on Peaceful Uses of Atomic Energy,* Vol 7, p 295, UN, Geneva, 1958

9 J M Davidson et al , HW57900 (Rev), 1959

10 D G Schweitzer and R M Singer, Radiation damage in graphite, II Kinetic reactions of interstitials, *J Chem Phys* , in press

## LIST OF BROOKHAVEN LECTURES

(Those with BNL numbers given have been published)

1. Radioastronomy and Communication Through Space, BNL 658
   Edward M. Purcell, Physics Department November 16, 1960
2. Current Ideas on the Endocrine Regulation of Cellular Processes, BNL 685
   Irving Schwartz, Medical Department December 14, 1960
3. Inside the Protein Molecule, BNL 649
   Werner Hirs, Biology Department January 11, 1961
4. Nuclear Chemistry Research With the Cosmotron
   Gerhart Friedlander, Chemistry Department February 15, 1961
5. Neutron Physics Of and With the High Flux Beam Research Reactor, BNL 664
   Herbert Kouts, Nuclear Engineering Department March 15, 1961
6. High Energy Accelerators, BNL 747
   Ernest Courant, Physics Department April 12, 1961
7. Dislocations in Crystal Lattices
   George H. Vineyard, Physics Department May 17, 1961
8. The History of Cosmic Rays in Meteorites
   Oliver A. Schaeffer, Chemistry Department June 14, 1961
9. The Physics of Semiconductor Radiation Detectors, BNL 699
   G.L. Miller, Instrumentation and Health Physics Department September 27, 1961
10. Theory of the Gene, BNL 739
    Milislav Demerec, Biology Department October 18, 1961
11. Fundamental Particles of Physics
    Maurice Goldhaber, Director, Brookhaven National Laboratory November 15, 1961
12. Excessive Salt Intake and Hypertension: A Dietary and Genetic Interplay, BNL 733
    Lewis K. Dahl, Medical Department December 13, 1961
13. Galaxies, BNL 710
    Otto Struve, National Radio Astronomy Observatory January 17, 1962
14. A Computer Learns To See, BNL 725
    Paul Hough, Physics Department February 14, 1962
15. Wet Electrons – The Radiation Chemistry of Water
    A.O. Allen, Chemistry Department March 14, 1962
16. Fundamental Studies of Radiation Damage in Graphite, BNL 745
    Donald G. Schweitzer, Nuclear Engineering Department April 17, 1962
17. The Role of the Cell Nucleus in Determining Radiosensitivity
    Arnold H. Sparrow, Biology Department May 16, 1962
18. Accelerators of the Future, BNL 741
    John P. Blewett, Accelerator Department June 13, 1962